JAERI - M
90-170

EFFECTS OF PRESSURE PROFILE AND PLASMA SHAPING ON THE n=1 INTERNAL KINK MODE IN JT-60/JT-60U PELLET FUELLED PLASMAS

October 1990

Takahisa OZEKI and Masafumi AZUMI

日 本 原 子 力 研 究 所
Japan Atomic Energy Research Institute

JAERI-Mレポートは，日本原子力研究所が不定期に公刊している研究報告書です。
入手の問合わせは，日本原子力研究所技術情報部情報資料課（〒319-11茨城県那珂郡東海村）あて，お申しこしください。なお，このほかに財団法人原子力弘済会資料センター（〒319-11 茨城県那珂郡東海村日本原子力研究所内）で複写による実費頒布をおこなっております。

JAERI-M reports are issued irregularly.
Inquiries about availability of the reports should be addressed to Information Division, Department of Technical Information, Japan Atomic Energy Research Institute, Tokai-mura, Naka-gun, *Ibaraki-ken* 319-11, Japan.

編集兼発行　日本原子力研究所
印　　刷　㈱原子力資料サービス

JAERI-M 90-170

Effects of Pressure Profile and Plasma Shaping on the n=1 Internal Kink Mode in JT-60/JT-60U Pellet Fuelled Plasmas

Takahisa OZEKI and Masafumi AZUMI

Department of Large Tokamak Research
Naka Fusion Research Establishment
Japan Atomic Energy Research Institute
Naka-machi, Naka-gun, Ibaraki-ken

(Received September 6, 1990)

The stability of the n=1 internal kink mode in a tokamak is numerically analyzed for plasmas with a centrally peaked pressure profile. These studies are carried out with the strongly peaked pressure inside the q=1 surface, which is based on the experimentally observed plasmas by means of injections of hydrogen-ice pellets in JT-60 tokamak. The effects of peaked pressure and shaping, i.e., elongation and triangularity, are also studied for JT-60U tokamak. The plasma with the strongly peaked pressure profile has higher critical value of poloidal beta defined within the q=1 surface than that with a parabolic pressure profile. Though the beta limit reduces with the increase of the elongation, the plasma with the peaked pressure profile has larger improvement due to the triangularity than that with the parabolic pressure profile. To access the second stability of the n=1 internal kink mode, the plasma with a flat pressure profile and the large minor radius of the q=1 surface is effective.

Keywords: Internal Kink Mode, n=1, Peaked Pressure Profile, MHD Stability, Pellet Injection, JT-60, JT-60U, Tokamak

JAERI－M 90－170

JT－60／JT－60Uペレット入射プラズマにおけるn＝1内部キンク安定性に対する圧力分布とプラズマ形状の効果

日本原子力研究所那珂研究所臨界プラズマ研究部
小関　隆久・安積　正史

（1990年9月6日受理）

中心ピークした圧力分布を持つプラズマのn＝1内部キンクモードの安定性を数値的に解析した。本研究では，JT－60 トカマクにおける水素ペレット入射実験で観測された，q＝1面内で強くピークした圧力分布を用いて解析を行った。また，ピークした圧力分布とプラズマ形状（すなわち，楕円度と三角度）の効果についても，JT－60 Uトカマクのために検討した。圧力が強くピークしたプラズマは，パラボリックな圧力分布を持つプラズマより，q＝1面内で定義されるポロイダルベータの限界値が高い。楕円度の増加によってこのポロイダルベータ限界値が下がるが，ピークした圧力分布を持つプラズマにおいては，三角度を付ける事によって大きな改善が得られる。一方，n＝1内部キンクの第2安定領域へアクセスするには，むしろ平坦な圧力分布で，q＝1面が大きいプラズマの方が効果的である事が示された。

那珂研究所：〒311－01 茨城県那珂郡那珂町大字向山801－1

Contents

目　　次

1. INTRODUCTION

Injections of Hydrogen-ice pellets are one of the attractive methods to enhance the fusion gain in a tokamak by making the centrally peaked pressure profile [1]. In pellet injection experiments of JT-60 [2], the confinement inside of the q=1 surface (q is the safety factor) was improved and the plasma pressure increased sharply in this region. The global energy confinement was enhanced up to 40% relative to usual gas fuelled discharges with neutral beam heating and the central value of the plasma pressure reached to 2 atoms at maximum, which was limited by the occurrence of the rapid m=1 activities. Theoretical analysis of ideal MHD stability has shown that the local pressure gradient in these discharges reached to the marginal value evaluated from the infinite-n ballooning stability, however the experimentally obtained total pressure was still lower than the optimized ballooning limit[3]. Instead of that, the results of the analysis of the kink instability showed that the beta limit of the n=1 internal kink mode had a good correlation with the attained maximum value of plasma pressure and with the occurrence of rapid m=1 activities [3]. Hence, the investigation of the property of the n=1 internal kink stability for the plasma with the peaked pressure profile is important to obtain the enhanced central values. In this paper, to analyze the stability, we use the equilibria observed in JT-60 as a example of the plasma with peaked pressure profile. Of particular interest are the effects of pressure profile shape and the plasma cross section on the stability boundary of n=1 internal mode for JT-60U tokamak [4].

The n=1 internal kink stability has been extensively studied by numerous authors. The stability condition of internal kink mode in a low beta tokamak with finite shear and circular cross section was first derived analytically by Bussac et al.[5] and this result was numerically confirmed

by means of ERATO code [6]. The reduction of the stability boundary for the low shear plasma and the onset of interchange-like instability was discovered by Nave and Wesson [7]. At high beta, the existence of a second stable region was numerically demonstrated by Tokuda et al.[8] and also analytically studied by Crew and Ramos [9]. The extensive numerical study of internal kink stability was carried out by Manickam in the wide range of parameters, such as aspect ratio, plasma shape, current profile, and pressure profile [10]. However, pressure profiles studied in these papers are assumed to have the rather smooth functional form. On the other hand, pressure profiles observed in pellet injection experiments in JT-60 show the highly peaked profile of plasma pressure only inside of the q=1 surface. Recent transport study shows that the suppression of the sawtooth oscillations and the good particle confinement inside of the q=1 surface are responsible to this type of pressure profile [11]. In a cylindrical plasma, only the pressure gradient inside of the q=1 surface contributes to the internal kink stability [12] and we can not expect the difference of stability criteria due to the pressure profile outside of the q=1 surface. In a toroidal system, however, the mode coupling effect takes the pressure gradient outside of the q=1 surface into the stability criterion and the centrally peaked pressure profile may have the different stability criterion from the conventional functional form of plasma pressure profile. Moreover, the usual analysis of MHD stability employs the so-called σ - scaling [13] for studying the safety factor dependence of the stability criterion. Tokamak experiments have shown that the position of the q=1 surface is inversely proportional to the safety factor at the plasma surface in the wide operation range, except in the current drive modes. Then we should keep this constraint of safety factor profile in mind, when we study the dependence of the stability boundary on the safety factor at the plasma axis.

In this paper, we numerically investigate the stability of the n=1 internal kink mode for the centrally peaked pressure profile in the wide range of parameters and reveal the effects of plasma profile and plasma shape. This paper is organized as follows; in the next section, numerical procedures of this study are explained and results of the effects of the pressure profile and the plasma shape are presented in section 3. In section 4, the access to the second stability regime of the n=1 internal kink mode is discussed. Section 5 is devoted to discussions and conclusions.

2. CALCULATION PROCEDURE

Key parameters to study the n=1 internal kink stability are the pressure profile and the current profile. Usually, the rather smooth functional form, like the squared parabolic profile, is employed as the pressure profile for the stability calculation. On the other hand, the pressure profiles obtained in pellet injection experiments in JT-60 have the different shapes; that is, the pressure increases only inside of the q=1 surface and the pressure gradient largely changes across this surface. This type of pressure profile can be well expressed in the following form;

$$P(\tilde{\psi}) = \frac{P_0}{1+\kappa}[1 - \tilde{\psi} + \kappa \cdot \exp\{-(\frac{\tilde{\psi}}{\delta})^{\nu}\}] \tag{1}$$

where $\tilde{\psi}$ is the poloidal flux function normalized such that $\tilde{\psi} = 0$ at the magnetic axis and $\tilde{\psi} = 1$ at the plasma surface. The subscript of 0 denotes the value of the magnetic axis. The last term in the bracket corresponds to the peaked part of the pressure profile and κ denotes the peaking factor. The parameter ν denotes the broadness of the peaked part and the parameter δ is chosen such that the steepest gradient of pressure is located just inside of the q=1 surface. In the following, we use $\nu = 4.0$ as the standard case because it well reflects the experimentally observed pressure gradient. For the comparison with this centrally peaked pressure profile, the squared parabolic pressure profile

$$P(\tilde{\psi}) = P_0(1 - \tilde{\psi})^2 \tag{2}$$

is also employed in the following calculations.

The surface averaged parallel current density is assumed to have the following profile;

$$< J_{\parallel} \cdot B >= \frac{J_0 B_0}{1+\sigma}\{(1 - \tilde{\psi}^{\alpha_1})^{\alpha_2} + \sigma\}, \tag{3}$$

In many tokamak experiments [14,15], it was found that the position of the q=1 surface, r_1, scales as $r_1 = a/q_a$, where a is the plasma minor radius

and q_a is the safety factor at the plasma surface, and this relation holds in the pellet injection experiments [2]. On the other hand, the q value at the plasma center, q_0, is not well measured. Thus, we carry out the scanning of q_0 with fixed surface q value and fixed radius of the q=1 surface. The current profile parameters, i.e., α_1, α_2 and σ, are adjusted from the q=1 surface ($r_1 = a/q_a$) for given total plasma current and q_0. Figure 1 shows the typical pressure profile and q-profile for several surface q-value.

The MHD equilibria with toroidal symmetry and up-down symmetry against the $Z = 0$ plane are obtained by solving the following Grad-Shafranov equation iteratively in the cylindrical co-ordinates (R, Z, φ) for prescribed current and pressure profiles.

$$R\frac{\partial}{\partial R}\left(\frac{1}{R}\frac{\partial \psi}{\partial R}\right) + \frac{\partial^2 \psi}{\partial Z^2} = \mu_0 R J_\varphi, \tag{4}$$

$$J_\varphi = -R\frac{dP}{d\psi} - \frac{1}{\mu_0 R}F\frac{dF}{d\psi}, \tag{5}$$

where ψ is the poloidal flux function, J_φ is a toroidal current density and μ_0 is permeability of vacuum. Since the internal kink mode is a weak instability, the accuracy requirements of the equilibrium and stability analysis are quite stringent. To ensure that these requirements are adequately met, we solve the equilibrium equation in the fine rectangular grid with N_R=512 in the R-direction and N_Z=256 in the Z-direction so that the ratio of the grid size to the average minor radius of the plasma is about 5×10^{-3}. The convergence criterion for the iteration of equilibrium calculation has been $\epsilon < 10^{-6}$, where ϵ is the maximum amplitude of the relative change between iterations. The two free functions, the $dP/d\psi$ and the toroidal field function $F(\psi)$, are specified by the pressure profile and the surface averaged parallel current $< J_\parallel >$ $(=< J_\parallel \cdot B > / < B >)$, respectively.

The stability of the n=1 internal kink mode is studied with the ideal linear stability code ERATO-J [16,17], which solves the linearized ideal

MHD equations in variational form using a finite hybrid element approach. This two-dimentional code computes the ideal MHD spectrum by minimizing the potential energy in the flux co-ordinate (ρ, χ), where $\rho = \sqrt{\bar{\psi}}$ and the poloidal angle χ is selected so that the magnetic field lines are straight.

The equilibria are mapped into a fine mesh with N_ρ up to 270 in the ρ direction and N_χ of 90 in the χ direction for analysis with the ERATO stability code, because a higher accuracy is required in the radial direction to examine the internal kink mode with the peaked pressure. The good offset linear dependence of the squared growth rate, $\hat{\gamma}^2$, against the squared radial grid mesh, N_ρ^2, is confirmed for every case by using the radial mesh number of 90 to 270 with equal spacing. Here the $\hat{\gamma}$ is the growth rate normalized by the Alfven velocity v_A and the major radius R_0 ($\hat{\gamma}^2 = \gamma^2/(v_A/R_0)^2$). The N_χ is fixed 90 because this poloidal mesh number is enough to calculate low n mode. We have taken the value of the $\hat{\gamma}^2$ (on $N_\rho \to \infty$) of 5×10^{-6} as the stability limit.

3. PRESSURE PROFILE AND PLASMA SHAPING EFFECTS

We study the effect of the peaked pressure profile on the n=1 internal kink mode stability in comparison with that of the squared parabolic profile. In the present paper, we use the experimentally observed parameter in JT-60 as a base equilibrium with circular configurations with $R = 3.05m$, $a = 0.9m$, $B_T = 4.8T$, $1.5MA \leq I_p \leq 3.1MA$ (B_T is the toroidal field, I_p is the plasma current). Effect of shaping is studied by changing elongation and triangularity from this base equilibrium up to non-circular configuration with $k = 1.8$ and $\delta = 0.25$. Since the purpose of this paper is to investigate the nature of the n=1 internal kink mode, we use the fixed boundary plasma.

First, we investigate the stability boundary for the peaked pressure profile plasmas, against the central q value. Thus, the q-profile is scanned by changing the q_0 with the fixed q=1 surface and fixed surface q, as shown in Fig. 2. The circular cross section is used to isolate the influence of geometry. Figure 3 shows the limited value of β_{p1} as a function of the q_0 for both the centrally peaked and squared parabolic pressure profile plasmas. Here, we use the poloidal beta defined within the q=1 surface, β_{p1}, which has been introduced by Bussac [5]

$$\beta_{p1} = \frac{2\mu_0}{B_p^2(r_1)} \int_0^{r_1} \left(\frac{r}{r_1}\right)^2 \left(-\frac{dP}{dr}\right) dr, \tag{6}$$

where r_1 is the minor radius of the q=1 surface. The stability boundary of the centrally peaked pressure profile is higher than that of the squared parabolic profile. The β_{p1} limit does not change so much as the q_0 decreases and no improvement is obtained on the contrary to the previous results by the σ-scaling [13]. We also observe that, when q_0 approaches to unity, the stability boundary of β_{p1} steeply decreases because the eigenfunction becomes interchange-like as pointed out by Nave and Wesson [7].

In the finite beta plasma, the destabilizing terms consist of pressure

driven and current driven components. These terms depend on the pressure and current profiles. Figure 4 shows contributions of the pressure driven term, W_{BALL}, and the current driven term, W_{KINK}, of the energy integral against the radial direction for both centrally peaked and squared parabolic pressure profiles with the same q-profile ($q_0 = 0.9$ and $q_s = 3.5$) and the same β_{p1} (≈ 0.62). The contribution of the current driven term on each pressure profile plasmas exhibits the same distribution because of the same q-profile (Fig. 4.e,f). In the plasma with the centrally peaked pressure profile, the contribution of the pressure driven term is concentrated within the q=1 surface (Fig. 4.c) and the sharp step-function like behaviour of ξ_r is evident (Fig. 4.a). In the parabolic pressure profile, the contribution of the pressure driven term is distributed inside and outside the q=1 surface (Fig. 4.d) and the amplitude of the eigenfunction outside the q=1 surface is larger than that of peaked profile (Fig. 4.b). The corresponding two dimensional plot of this eigenvector are shown in Fig. 5. Because these both plasmas is adjusted to have the same amount of β_{p1}, the squared parabolic pressure profile has the same contribution of the pressure driven term within the q=1 surface as the peaked one has. However, the parabolic profile plasma has larger contribution of the pressure driven term from outside of the q=1 surface by the mode coupling. Therefore, the total pressure driven component is larger than that of the peaked pressure profile, and the stability boundary of β_{p1} is lower than that of the peaked pressure profile.

Next, we extend the study to the non-circular plasma. In the future tokamak, e.g. JT-60U, the shape of the poloidal cross-section will be elongated and be made to have a week triangularity. Hence, it is important to examine the effect of the elongation and triangularity on the peaked pressure profile plasmas. A sequence of equilibria is examined with the

elongation varying from $\kappa = 1.0$ to $\kappa = 1.8$ while keeping the total current and the q_0 fixed. Triangularity is kept fixed to $\delta = 0$ or $\delta = 0.25$. Generally, the internal kink mode is destabilized by the elongation and is stabilized by the triangularity[10]. Figure 6.a shows the limited value of β_{p1} against the elongation with and without triangularity for the squared parabolic pressure profile plasma. The increase of elongation reduces the β_{p1} limit, while the stability is slightly improved by the triangularity. These results confirm the previous results[10]. For the centrally peaked pressure profile, the β_{p1} limit also decrease with the increase of the elongation. However, when the triangularity is added, a larger improvement of the stability boundary is obtained as shown in Fig. 6.b. Figure 7 shows contributions of the pressure driven term, W_{BALL}, and the current driven term, W_{KINK}, for the corresponding pressure profiles in Fig. 6 ($\kappa = 1.6$ and $\delta = 0.25$). Each pressure profile has the same q_0 of 0.95, the same r_1/a of 0.33 and the same β_{p1} of ≈ 0.45. In both types of plasma, the contribution of the pressure driven term becomes broad as the elongation increases (Fig. 7.c,d), compared with the circular one shown in Fig. 4. Especially in the parabolic pressure profile, the contribution of the pressure driven term largely spreads both inside and outside the q=1 surface (Fig. 7.d) and the eigen function is mixed by the higher modes (Fig. 7.b). The corresponding two dimensional plot of the eigenvector is shown in the squared parabolic pressure case (Fig. 8.b), where the vortex rotates around the magnetic axis with a convective feature. This figure shows that the contribution of the pressure driven term is larger due to the larger mode coupling than the peaked pressure profile case. Therefore, the squared parabolic profile plasma has lower critical β_{p1} boundary against the n=1 internal kink mode.

4. ACCESS TO THE SECOND STABILITY

In the previous papers based on the σ scaling analysis [13], the second stability region of the n=1 internal kink mode was theoretically demonstrated by the decrease of q_0. For the JT-60 operation regime, i.e., $q_s > 2.2$ and $r_1/a < 0.45$, the plasma can not access to the second stability region of the n=1 internal kink mode, as shown in Fig. 3. The decrease of the q_0 by the σ-scaling keeps the q-profile fixed and increases the minor radius of the q=1 surface. Thus, we try to increase the minor radius of the q=1 surface over the experimentally observed value. Figure 9 shows the stability boundary for the plasma with the large minor radius for $r_1/a = 0.67, 0.78$. When the r_1/a becomes over the value of 0.78, the stability region in the β_{p1}-q_0 space drastically spreads without the small region near $q_0 = 0.9$. According to the analysis of Crew and Ramos [9], the access to the second stability is caused by deepening the magnetic well due to the shift of the magnetic axis. Figure 10 shows the value of the shift of the axis in the $\beta_p - r_1/a$ plane. The plasma with the larger r_1/a has the larger shift of the magnetic axis for the same value of β_p. Therefore, the plasma with large r_1/a is effective to access the second stability.

In the present paper, the plasma with the centrally peaked pressure profile with high β_{p1} and low β_p is considered, i.e., a high value of β_{p1}/β_p represents the peaked pressure profile. The accessibility to the second stability region in the $\beta_{p1}/\beta_p - r_1/a$ plane is examined, as shown in Fig. 11. When the ratio of β_{p1}/β_p is small, the plasma can easily access to the second stability regime. This is because, when the β_p increase keeping the ratio of β_{p1}/β_p low, the magnetic well stabilization can become large before the pressure driven term within the q=1 surface destabilizes the n=1 internal kink mode. Therefore, the low β_{p1}/β_p and the large r_1 can easily access to the second stability region, so that the strongly peaked

one is not effective for the access to the second stability.

5. DISCUSSION

In the JT-60U tokamak, the pellet injection experiments will be also carried out to obtain the enhanced central parameter, n_{e0}, T_{e0} and τ_e. However, from the analysis of JT-60 pellet fuelled experiments[3], the peaked pressure within the q=1 surface is limited by the internal kink mode. Thus, we discuss the critical β_{p1} in the typical configurations of JT-60U from the results of section 3. In JT-60U, the poloidal field coil system is designed to produce D-shape limiter and divertor plasmas with various plasma elongations[4]. The typical plasma configurations are shown in Fig. 12. In the elongated divertor mode, the plasma will have the high elongation ($k = 1.8$) and no triangularity ($\delta = 0$). The critical β_{p1} in the elongated divertor mode is reduced by one-third of the critical β_{p1} of the circular cross-section plasma. Therefore, the highly peaked pressure profile in the elongated divertor mode can not be produced even by a good pellet penetration and a high NB injection power. On the other hand, in the limiter mode ($k = 1.4$ and $\delta = 0.16$) or the standard divertor mode ($k = 1.5$ and $\delta = 0.19$), the plasmas will have elongation and have not large positive triangularity. Therefore, the reduction of critical β_{p1} due to the elongation remained two-third of the critical β_{p1} of the circular cross-section plasma. And also, the peaked pressure profile plasma has the large improvement of the critical β_{p1} by adding the triangularity. Thus, in the limiter mode or the standard divertor mode, the relatively peaked pressure profile can be produced than that of the elongated divertor mode. Furthermore, if they can produce the slightly elongated plasma ($k \approx 1.5$) with the larger triangularity ($\delta > 0.25$), the strongly peaked pressure profile, which is

same as the obtained plasma in the circular plasma of JT-60, will be obtained.

6. SUMMARY

The n=1 internal kink stability for the plasma with strongly peaked pressure profile within the q=1 surface is investigated, where the equilibrium is based on the experimentally observed plasma in JT-60 pellet fuelling experiments, i.e., the confinement inside the q=1 surface was improved and that outside the q=1 surface remained L-mode. The results of the numerical study by means of ERATO-J code show that the plasma with peaked pressure profile has higher critical β_{p1} against the n=1 internal kink mode than that of the squared parabolic profile.

We extend the study from the base equilibria with the circular cross-section to those with the non-circular one. The plasma with a peaked pressure profile has larger improvement due to the increase of triangularity than that with the squared parabolic pressure profile . In the future tokamak, e.g. JT-60U, with the elongated poloidal shape, therefore, a strongly peaked plasma can reduce the degradation of the β_{p1} limit by adding the triangularity.

When rearranging the calculation results, the plasma with the peaked pressure profile, i.e., high value of β_{p1}/β_p, is preferable to increase the first stability boundary due to the week of the mode coupling, while the plasma with low value of β_{p1}/β_p and the large r_1 is preferable to access the second stability due to the large magnetic well. In the JT-60 operation regime of pellet injecting experiments, the β_{p1}/β_p went up to about 2, and the minor radius of r_1/a could not be increased over ~ 0.5. Consequently, the current

profile control is necessary to access the second stability regime.

ACKNOWLEDGEMENTS

The authors would like to express their gratitude to Drs. S.Tokuda and T.Tsunematsu for their fruitful discussion and for the use of ERATO-J code. They are also grateful to the members of JT-60 team and Drs. M.Yoshikawa, M.Tanaka, T.Iijima, S.Tamura and Y.Shimomura for their continuous support and encouragement.

REFERENCES

[1] M. Kaufmann: Plasma Phys. Controll. Fusion 28 (1986) 1341.

[2] Y. Kamada, R. Yoshino, M. Nagami, T. Ozeki, T. Hirayama, H. Shirai, H. Nakamura, H. Kimura, T. Fujii, K. Kawasaki, H. Hiratsuka, Y. Miyo, K. Nagashima, H. Yoshida and T. Nishitani: Nucl. Fusion 29 (1989) 1785.

[3] T. Ozeki, M. Azumi, Y. Kamada, R. Yoshino, S. Tokuda, T. Tsunematsu, K. Nagashima, H. Yoshida and M. Nagami: submitted for Nucl. Fusion. (or JT-60 Team: Review of JT-60 experimental results from January to October, 1989, Rep. JAERI-M 90-066 Japan Atomic Energy Research Institute, Ibaraki (1990) 16.)

[4] M.Kikuchi, T.Ando, M.Araki, et al.: Fusion Technology, Pergamon Press, Oxford, 1 (1989) 287.

[5] M.N.Bussac, R.Pellat, D.Edery and J.L.Soule: Phys. Rev. Lett. 15 (1975) 1638.

[6] W.Kerner, R.Gruber and F.Troyon: Phys. Rev. Lett. 25 (1980) 536.

[7] M.F.F. Nave and J. Wesson: Nucl. Fusion 28 (1988) 297.

[8] S. Tokuda, T. Tsunematsu, M. Azumi, T. Takizuka and T. Takeda: Nucl. Fusion 22 (1982) 661.

[9] G.B.Crew and J.J.Ramos: Phys. Rev. A 26 (1982) 1149.

[10] J.Manickam: Nucl. Fusion 24 (1984) 595.

[11] K.Shimizu: private communication.

[12] M.N. Rosenbluth, R.Y. Dagazian and P.H. Rutherford: Phys. Fluids 16 (1973) 1894.

[13] R. Gruber, F. Troyon, D. Berger, L. C. Bernard, S. Rousset, R. Schreiber, W. Kerner, W. Schneider and K. V. Roberts, Comput. Phys. Commun. 21 (1981) 323.

[14] R.J. Goldstone: Plasma Phys. Controll Fusion 26 (1984) 87.

[15] JT-60 Team: in Plasma Physics and Controlled Nuclear Fusion Research 1986 (Proc. 11th Int. Conf. Kyoto, 1986) Nucl. Fusion, Vol. 1, (1987) Suppl. 217.

[16] Y. Tanaka, T. Matsuura, T. Takeda, M. Azumi, S. Tokuda, T. Tsunematsu, G. Kurita and T. Takizuka: MHD Stability Analysis Code ERATO-J, Rep. JAERI-M 9040, Japan Atomic Energy Research Institute, Ibaraki (1980) [in Japanese].

[17] S. Tokuda, T. Tsunematsu, M. Azumi, T. Takizuka, K. Naraoka and T. Takeda: MHD Stability Analysis by Revised Version of ERATO-J, Rep. JAERI-M 9899, Japan Atomic Energy Research Institute, Ibaraki (1982) [in Japanese].

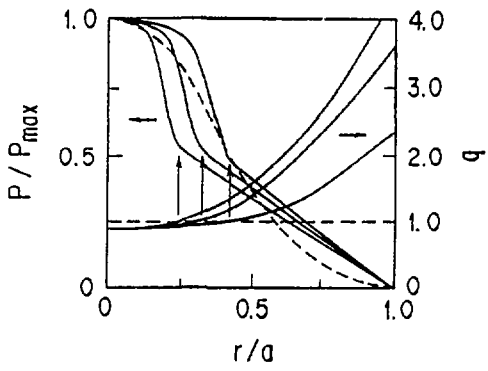

Fig. 1 Pressure profile and q-profile for various surface q, which are based on the pellet fuelling experiments in JT-60. Broken line shows the squared parabolic pressure profile.

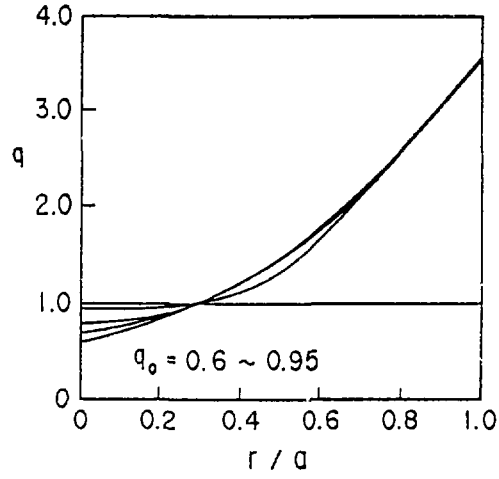

Fig. 2 q-profiles used for the q_0-scanning in the stability calculation.

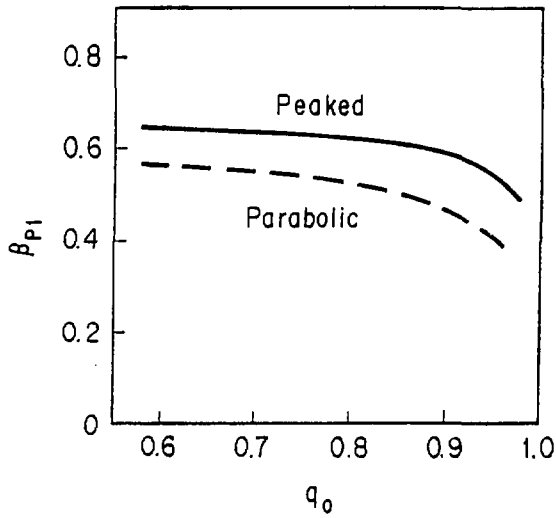

Fig. 3 Comparison of critical βp_1 of the peaked pressure profile (ν=4.0, δ=0.1, κ=0.6; Solid line) with that of the squared parabolic pressure profile (Broken line). Above the each line, the n=1 internal kink mode is unstable.

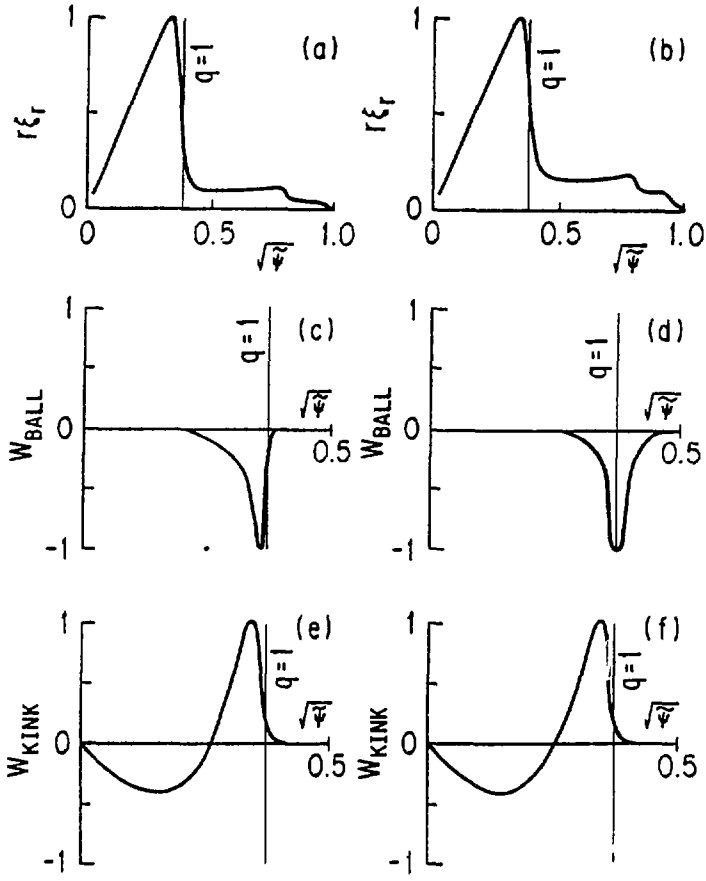

Fig. 4 Radial dependence of the normal displacement $r\xi_r$, the normalized pressure driven term W_{BALL} and the normalized current driven term W_{KINK} for the peaked pressure profile ((a),(c),(e)) and for the squared parabolic pressure one ((b),(d),(f)). These plasmas correspond to those with q_0=0.9, q_s=3.5 and βq_1=0.63 in Fig. 3.

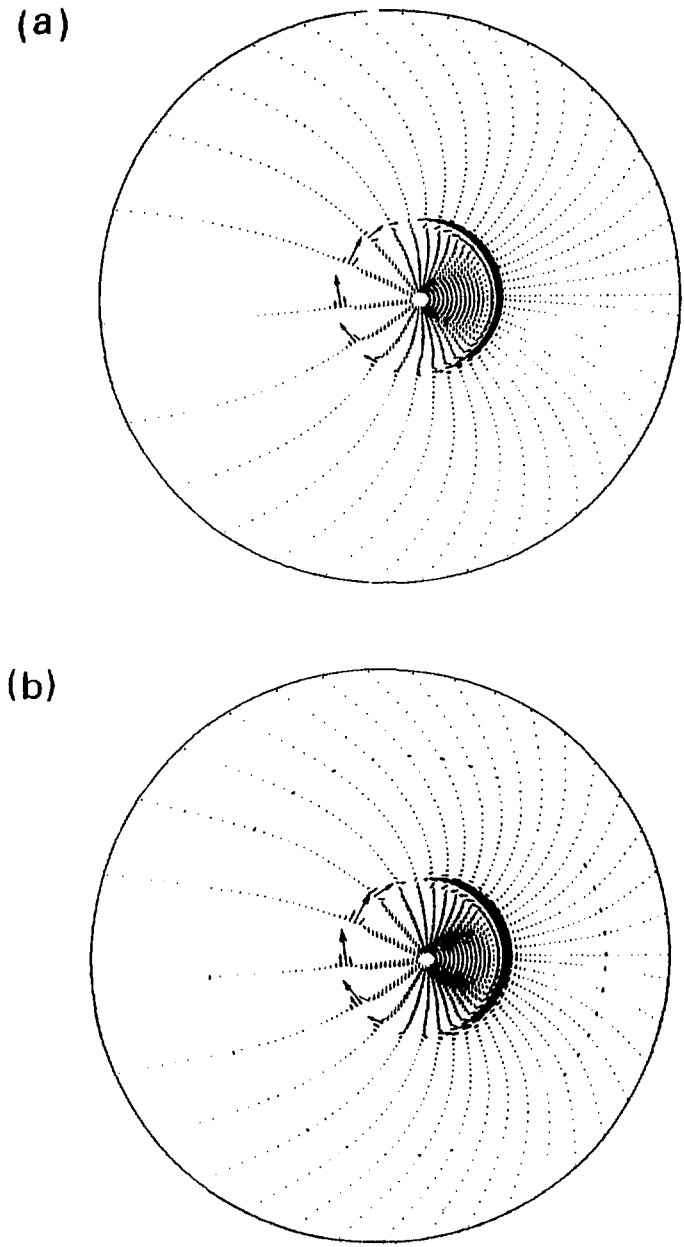

Fig. 5 Displacement vector of the poloidal component for (a) the peaked pressure plasma and (b) the squared parabolic pressure one in Fig. 4.

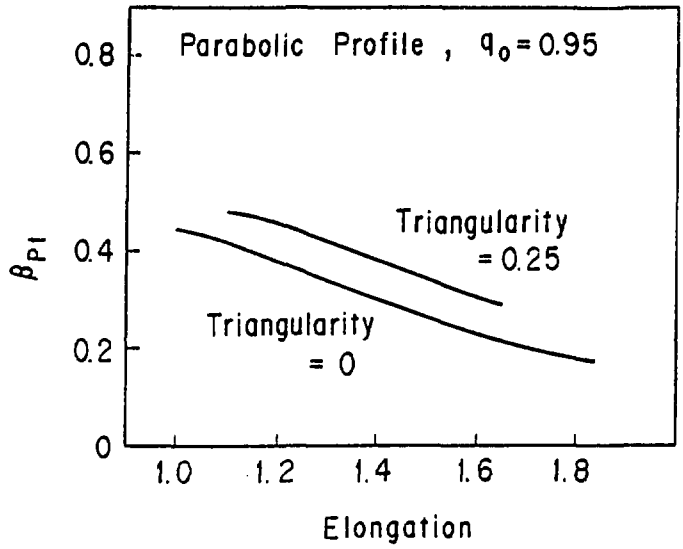

Fig. 6.a Dependency of critical βp_I of the squared parabolic pressure profile on the elongation and triangularity.

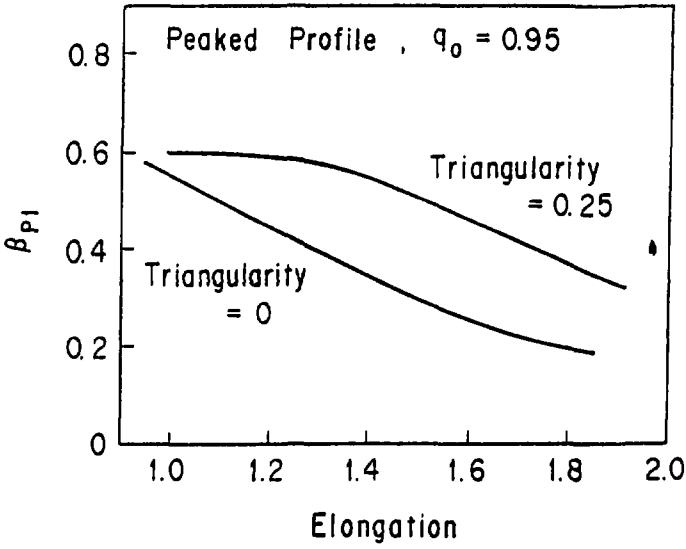

Fig. 6.b Dependency of critical βp_I of the peaked pressure profile (ν=4.0, δ=0.1, κ=0.6) on the elongation and triangularity.

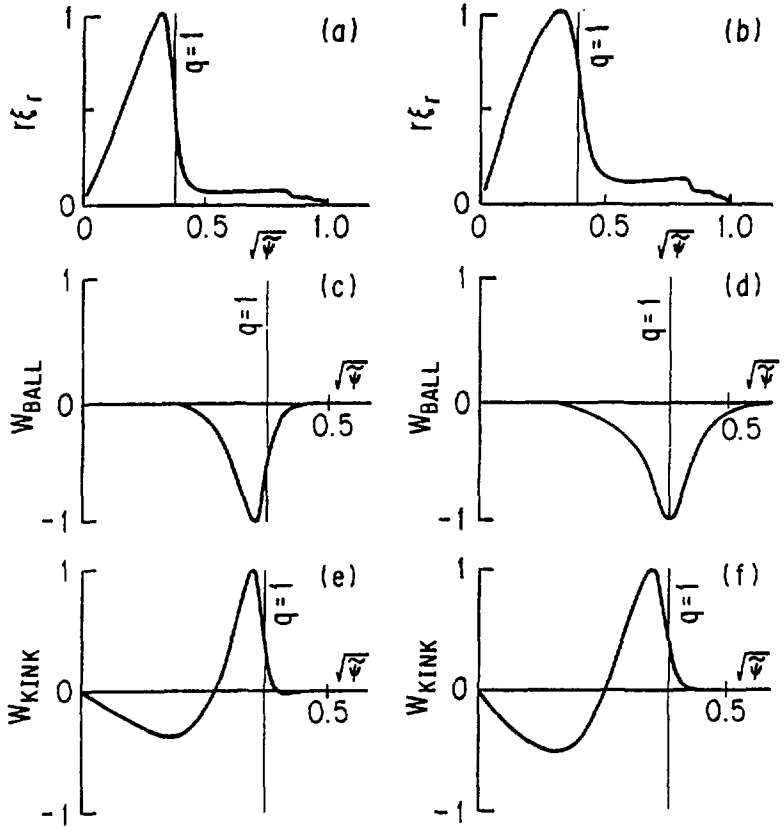

Fig. 7 Radial dependence of the normal displacement $r\xi_r$, the normalized pressure driven term W_{BALL} and the normalized current driven term W_{KINK} for the peaked pressure profile ((a),(c),(e)) and for the squared parabolic pressure one ((b),(d),(f)) in non-circular plasmas with $k=1.6$, $\delta=0.25$, $q_0=0.95$ and $\beta p_l=0.45$.

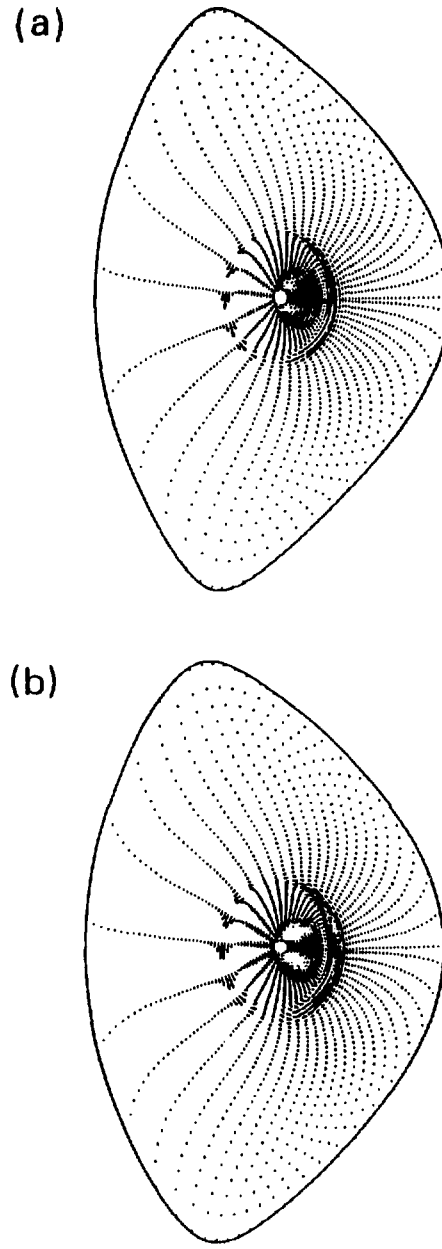

Fig. 8 Displacement vector of the poloidal component for (a) the peaked pressure plasma and (b) the squared parabolic pressure one in Fig. 7.

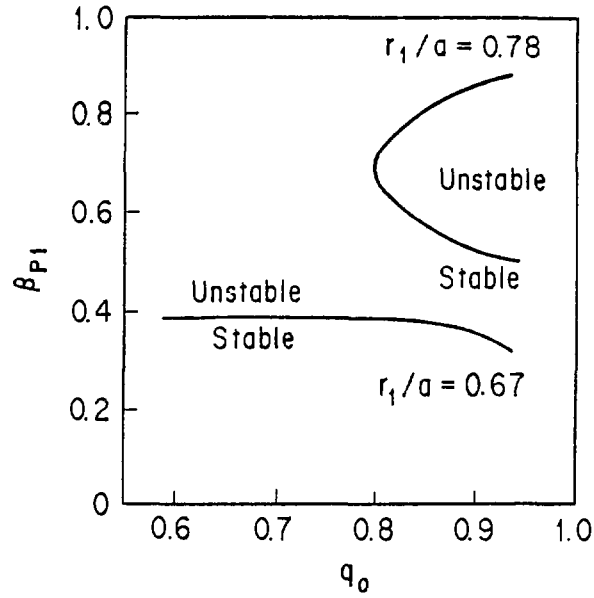

Fig. 9 Stability boundary on the βp_1 - q_0 plane for the different r_1 values, i.e., r_1/a=0.78, $\beta p_1/\beta p$= 0.45 and r_1/a=0.67, $\beta p_1/\beta p$=0.75.

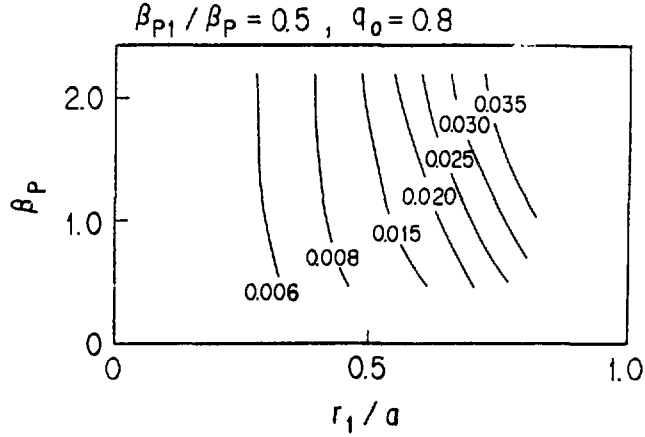

Fig. 10 Contour of the axis shift for the q=1 surface when q_0=0.8, q_s=2.2 and $\beta p_1/\beta p$=0.5. The shift is given by $R_{axis}-R_c$, where R_c is the geometric center of the q=1 surface.

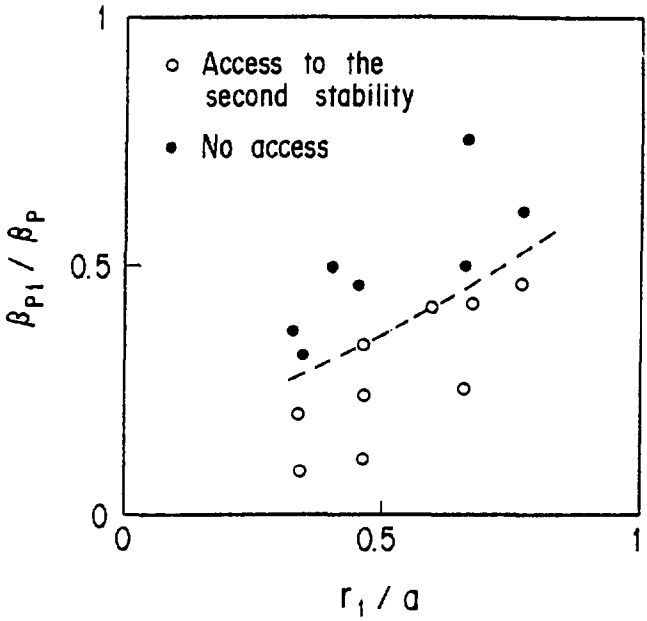

Fig. 11 Dependence of $\beta p_1/\beta p$ and r_1/a on the access to the second stability regime.

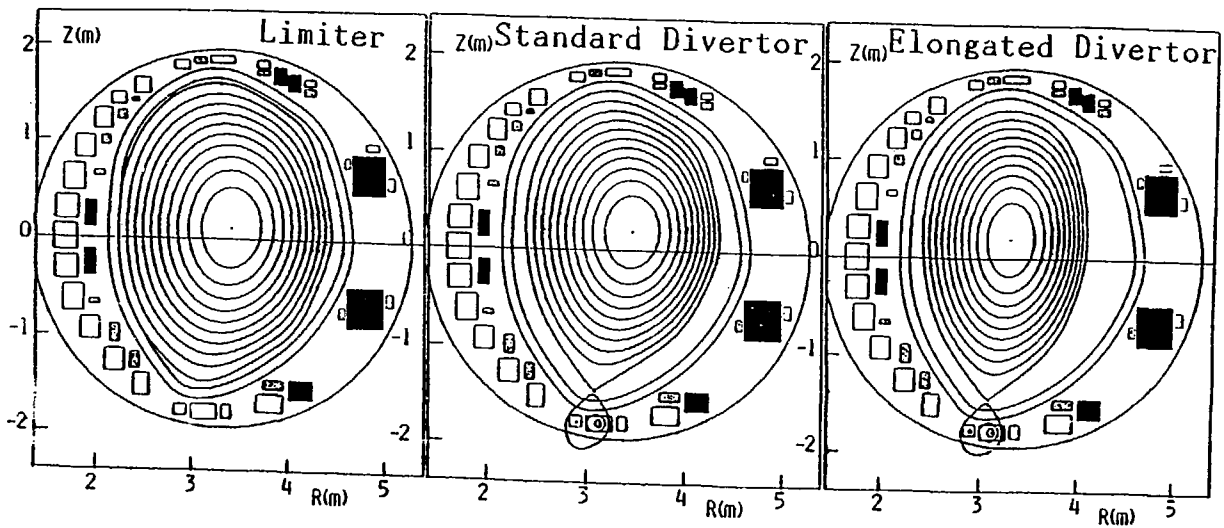

Fig. 12 Typical equilibria in JT-60U; Limiter mode (k=1.4, δ=0.16), Standard divertor mode (k=1.5, δ=0.19), Elongated divertor mode (k=1.8, δ=0)